Available online at www.sciencedirect.com

SCIENCE DIRECT®

ELSEVIER

Journal of Nuclear Materials 337–339 (2005) 301–304

journal of nuclear materials

www.elsevier.com/locate/jnucmat

Modelling and consequences of drift effects in the edge plasma of Alcator *C*-Mod

X. Bonnin [a,*], D. Coster [b], R. Schneider [a], D. Reiter [c], V. Rozhansky [d], S. Voskoboynikov [d]

[a] *Max-Planck-Institut für Plasmaphysik, Teilinstitut Greifswald, EURATOM Association, D-17491 Greifswald, Germany*

[b] *Max-Planck-Institut für Plasmaphysik, EURATOM Association, D-85748 Garching, Germany*

[c] *Institut für Plasmaphysik, Forschungszentrum Jülich GmbH, EURATOM Association-KFA, Trilateral Euregio Cluster, D-52425 Jülich, Germany*

[d] *Saint Petersburg State Technical University, 195251 St. Petersburg, Russia*

Abstract

We model the plasma edge of Alcator *C*-Mod with the B2-Eirene SOLPS5.0 code. The drifts, currents and neutral effects contribute to strong plasma rotation in the edge, as measured experimentally [B. LaBombard, S. Gangadhara, B. Lipschultz, C.S. Pitcher, J. Nucl. Mater. 313–316 (2003) 995; B. LaBombard, N. Smick, B. Lipschultz, J.L. Terry, J. Rice, these Proceedings; N. Smick, B. LaBombard, C.S. Pitcher, these Proceedings]. The plasma flow patterns are a complex superposition of several competing effects, including Pfirsch–Schlüter flows and currents, toroidal momentum generation and transport (with main chamber neutral recycling and drag playing an important role), as well as the $\mathbf{E}\times\mathbf{B}$ and diamagnetic drift flows. In the standard field direction the $\mathbf{E}\times\mathbf{B}$ flow in the core region adds to the toroidal plasma rotation, while in the reverse direction their respective contributions are roughly of the same order of magnitude but with opposite signs in the plasma core. However, in the edge, all terms can be of the same sign over most if not all of the radial extent of the SOL, leading to complex patterns and very strong flows.
© 2004 Elsevier B.V. All rights reserved.

PACS: 52.25.Fi; 52.30.−q; 52.55.Fa; 52.65.−y
Keywords: Edge modelling; Alcator *C*-Mod; B2-Eirene; Particle drifts; *B*-field reversal

1. Motivation

Langmuir probes at the edge of diverted tokamak plasmas routinely measure very large plasma flows, with Mach numbers reaching 0.5 to unity far away from any solid surface [1–6]. Additional experiments carried out in reversed field (with the $\mathbf{B}\times\nabla\mathbf{B}$ direction pointing away from the divertor *X*-point) distinguish between flow components varying with the magnetic field direction, as expected from neoclassical drifts, and field-independent background flows. In addition to the drifts, namely $\mathbf{E}\times\mathbf{B}$, diamagnetic, $\mathbf{B}\times\nabla\mathbf{B}$ and curvature drifts, other contributing effects have been invoked to explain measured flows, for example ion-orbit losses [7], anomalous convective transport [8] or pinches [9], ballooning-like

* Corresponding author. Address: Association EURATOM-CEA, CEA/DSM/DRFC, CEA Cadarache, F-13108 Saint-Paul-lez-Durance CEDEX, France. Tel.: +33 1 49 40 34 11; fax: +33 1 49 40 34 14.

E-mail address: bonnin@limhp.univ-paris13.fr (X. Bonnin).

0022-3115/$ - see front matter © 2004 Elsevier B.V. All rights reserved.
doi:10.1016/j.jnucmat.2004.10.102

transport [2,4,5,8,9], toroidal rotation [1], or possibly plasma acceleration towards the probe body during the measurement [4,5].

In this paper, we build on previous work done to simulate the edge plasmas of Alcator *C*-Mod [10] with the B2-Eirene SOLPS5.0 (Scrape-Off Layer Plasma Simulation) code [11–13]. The Alcator *C*-Mod case is particularly interesting because its compact size and strong field tend to produce strong drift effects. We show that the complex flow pattern observed can only be understood through a synergy of all drift effects included.

2. Simulation parameters

The B2-Eirene SOLPS5.0 code [11–13] solves the plasma continuity equations (particle, parallel momentum and ion and electron energy conservation) in the fluid approximation, following Braginskii [14], coupled with a Monte-Carlo model for the neutrals. Additionally, the current continuity equation ($\nabla \bullet \mathbf{J} = 0$) is solved, yielding the electric potential. In the version used here, neither the centrifugal force term nor the perpendicular current terms due to the heat flux components of the viscosity tensor, perpendicular viscosity or ion-neutral friction (the $\ln h_z$ terms and Eqs. (18), (19) and (21) of Ref. [13], respectively), are implemented. We consider a deuterium-only plasma because of uncertainties on the location and strengths of any carbon sources (or other low-Z impurities) in a molybdenum machine such as Alcator *C*-Mod.

We will consider both field directions, varying the core electron density n_e^{core} via a fixed core boundary condition. Any neutrals penetrating this far are ionized in the core plasma and re-injected at the core boundary as ions, with a poloidally uniform distribution. By setting recycling coefficients of 99.9% at the targets surface, we allow a small amount of pumping to take place to balance the particle influx at the core. The heating power is set to 1.1 MW, evenly split between the ion and electron channels. For numerical stability reasons, a feedback scheme is used that finds the ion and electron temperatures (T_e and T_i), constant on the core boundary, yielding the imposed heat input. In accordance with experiment, there is no momentum input into the plasma core.

3. Results and analysis

We present in Figs. 1 and 2 the parallel flow Mach numbers obtained for the middle and high density cases in both field directions along the inner (Fig. 1) and outer (Fig. 2) midplane of Alcator *C*-Mod. In all cases, there is a strong SOL flow across the inner midplane, always directed towards the inner divertor, which depends little on either plasma density or field direction. The situation along the outer midplane is more complex. With reversed field, the SOL plasma flow is directed towards the outer divertor. In normal field, only the outermost radii show a flow towards the outer divertor, while the region closer to the separatrix shows flow towards the inner divertor. Thus, the position of the poloidal stagnation point varies with radius and field. In normal field, it is actually located near the *X*-point on the separatrix and moves away from the (outer) divertor as radius increases, eventually crossing the outer midplane. In reversed field, the stagnation point is near the top of the machine across the entire SOL width. These trends show little density dependence.

As reported in [2], in normal field, a Mach number profile rising linearly from $M_\parallel \sim 0$ to almost $M_\parallel = 1$

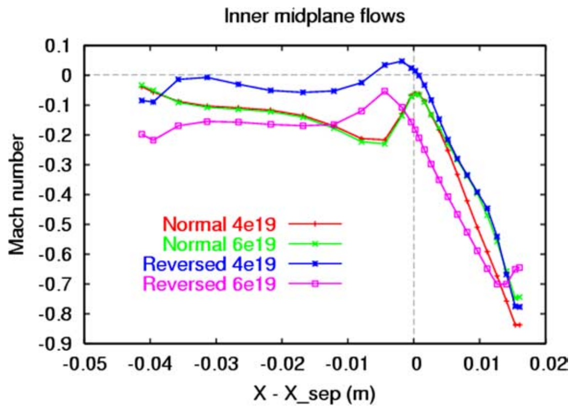

Fig. 1. Mach number profiles along the equatorial inner midplane of Alcator *C*-Mod, for both field directions and $n_e^{core} = 4$ or $6 \times 10^{19}\,\mathrm{m}^{-3}$, as a function of distance to the separatrix along the midplane. The core plasma is to the left of the figure. Negative Mach numbers indicate flows directed towards the inner divertor.

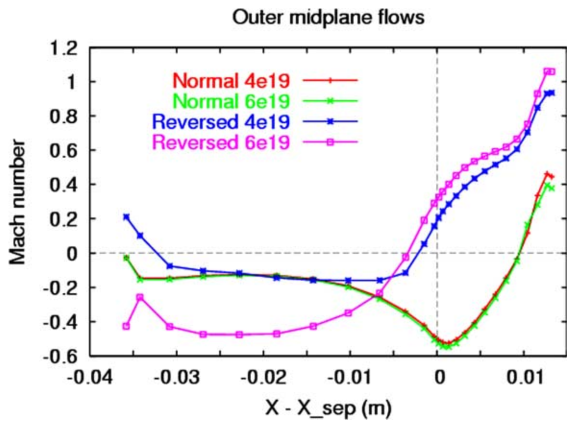

Fig. 2. Mach number profiles along the equatorial outer midplane of Alcator *C*-Mod, for both field directions and $n_e^{core} = 4$ or $6 \times 10^{19}\,\mathrm{m}^{-3}$. Same conventions as Fig. 1.

across the $\sim$ 1 cm SOL width and much smaller values, only reaching $M_{\parallel} \sim 0.2$ along the outer midplane, in both cases directed towards the inner divertor, are measured. In a geometry somewhat similar to our reversed field configuration, measurements indicate near stagnant flow at the outer midplane, but strong flows ($M \sim 0.5$–1.0) at the inner midplane throughout the SOL width. Because the details of the discharges and magnetic configurations between the cases studied here and those of Ref. [2] are different, only qualitative comparisons can be made, but dedicated simulations for cases such as in [2] are under way.

The simulated flow pattern can be understood in terms of a combination of neutral recycling patterns and, to a lesser extent, $\mathbf{E} \times \mathbf{B}$ effects. First, the simulations show that a fraction of the recycled neutrals escape the divertor and cross the separatrix back into the main plasma on the inner side of the *X*-point, because of its closeness to the wall and tendency to achieve more detached conditions, while almost no ionization occurs on the LFS of the confined region. Second, the presence of a potential hill located at the *X*-point induces a plasma circulation around it, contrary to the no-drifts pattern of plasma flowing mostly along field lines. In normal field, this flow goes around the *X*-point in the clockwise direction, that is promotes plasma flow from outer to inner divertor below the *X*-point and hence enhances the recycling efficiency on the inner side of the *X*-point. In reversed field, this flow is counter-clockwise and goes against the plasma tendency to establish a flow from outer to inner divertor in the SOL. Such $\mathbf{E} \times \mathbf{B}$ flows, in normal field, also have a stabilizing influence against density instabilities like *X*-point MARFEs, by forcing plasma flow that would otherwise be flowing towards the *X*-point to flow around it, while they likely contribute to higher H-mode thresholds in reversed field.

In Figs. 3 and 4, we show the various contributions to the poloidal flow velocity, defined as the particle flow between two poloidally neighbouring computational cells divided by their average density and area of contact. The contribution noted '**Dia**' contains the divergent part of the usual diamagnetic terms only, that is,

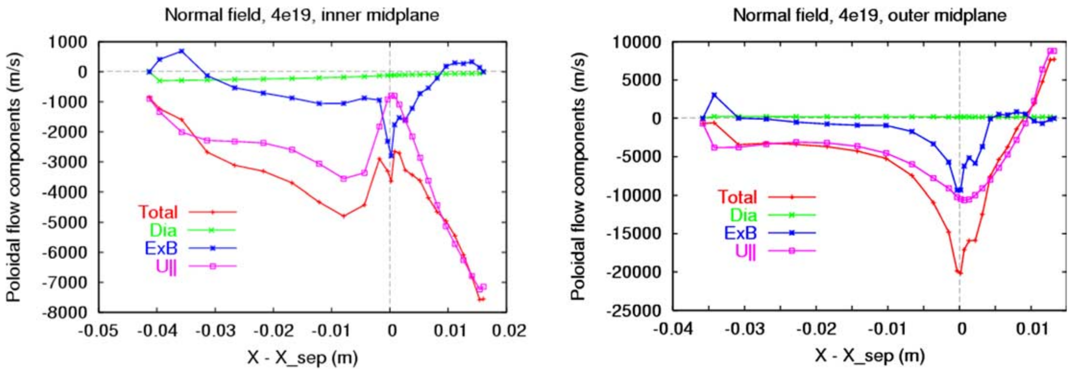

Fig. 3. Individual components of the poloidal velocity along the inner (left) and outer (right) midplane for the $n_e^{core} = 4 \times 10^{19}\ m^{-3}$ case with normal field direction. Same convention as in Fig. 1.

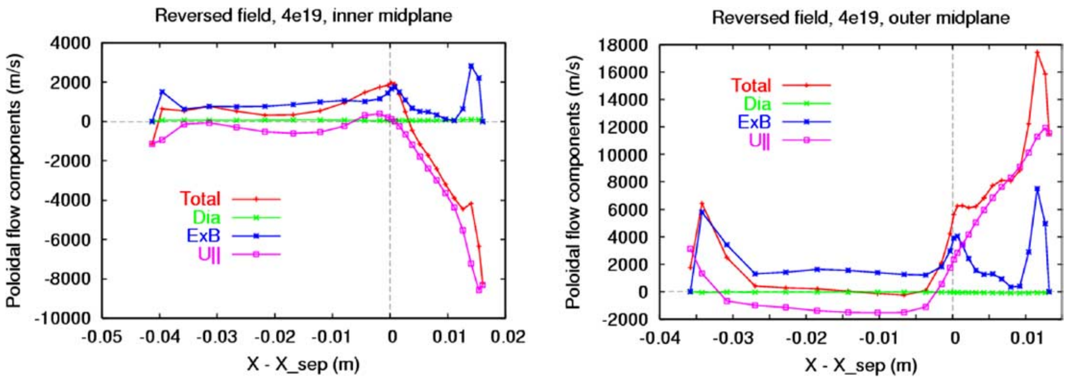

Fig. 4. Individual components of the poloidal velocity along the inner (left) and outer (right) midplane for the $n_e^{core} = 4 \times 10^{19}\ m^{-3}$ case with reversed field direction. Same convention as in Fig. 1.

proportional to $T_i \nabla B^{-2}$ [11–13], the '$\mathbf{E}\times\mathbf{B}$' term is the poloidal component of the $\mathbf{E}\times\mathbf{B}$ velocity and '$U_{\|}$' is the poloidal projection of the parallel velocity, as obtained from the solution of the parallel momentum equation (including the consequences of drift terms). In all cases, the '**Dia**' contribution is negligible by itself, but the inclusion of diamagnetic effects establishes a large radial electric field inside the core plasma, which in turn will drive significant core $\mathbf{E}\times\mathbf{B}$ flows in the diamagnetic direction. In normal field, the major contribution remains the poloidal projection of the parallel velocity, once again pointing to toroidal rotation as the main flow mechanism, except near the separatrix, where strong $\mathbf{E}\times\mathbf{B}$ flows can be present in the shear layer between the confined plasma and the SOL, as expected from Pfirsch–Schlüter physics.

4. Conclusions

We have presented a series of B2-Eirene SOLPS5.0 simulations of the Alcator *C*-Mod edge plasma, including drift and current effects. The SOL flow patterns and trends under field reversal are roughly consistent with experimental measurements, although more focused comparisons are needed and ongoing. Under normal conditions, a strong SOL flow exists directed towards the inner divertor. This flow is more balanced with reversed field. The complex pattern of flows can only be explained when one considers the synergies of recycling, Pfirsch–Schlüter physics, diamagnetic and $\mathbf{E}\times\mathbf{B}$ flows.

Acknowledgments

The authors would like to thank A. Chankin of IPP-Garching for insightful physics discussions. The kind collaboration of B. LaBombard and C.S. Pitcher of the Alcator *C*-Mod team at MIT for providing access to the experimental data is gratefully acknowledged. This work is supported in part by INTAS Project #457.

References

[1] B. LaBombard, S. Gangadhara, B. Lipschultz, C.S. Pitcher, J. Nucl. Mater. 313–316 (2003) 995.
[2] B. LaBombard, N. Smick, B. Lipschultz, J.L. Terry, J. Rice, 16th Int. Conf. on Plasma–Surface Interactions in Controlled Fusion Devices, Portland, Maine, USA, 2004, paper I-5.
[3] N. Smick, B. LaBombard, C.S. Pitcher, these Proceedings. doi:10.1016/j.jnucmat.2004.09.035.
[4] R. Pitts, P. Andrew, X. Bonnin, A.V. Chankin, Y. Corre, et al., these Proceedings. doi:10.1016/j.jnucmat.2004.10.111.
[5] S.K. Erents, R.A. Pitts, W. Fundamenski, J.P. Gunn, G.F. Matthews, Plasma Phys. Control. Fus. 46 (2004) 1757.
[6] N. Asakura, H. Takenaga, S. Sakurai, H. Tamai, A. Sakasai, et al., Plasma Phys. Control. Fus. 44 (2002) 2101.
[7] W. Fundamenski, S. Sipilä, T. Eich, T. Kiviniemi, T. Kurki-Suomo, et al., J. Nucl. Mater. 313–316 (2003) 787.
[8] A.Yu. Pigarov, S.I. Krasheninnikov, T.D. Rognlien, M.J. Schaffer, W.P. West, Phys. Plasmas 9 (2002) 1287.
[9] G. Kirnev, G. Corrigan, D. Coster, S.K. Erents, W. Fundamenski, et al., these Proceedings. doi:10.1016/j.jnucmat.2004.09.032.
[10] X. Bonnin, D. Coster, C.S. Pitcher, R. Schneider, D. Reiter, et al., J. Nucl. Mater. 313–316 (2003) 909.
[11] R. Schneider, D. Coster, B. Braams, P. Xantopoulos, V. Rozhansky, et al., Contribution Plasma Phys. 40 (2000) 328.
[12] V. Rozhansky, S. Voskoboynikov, E. Kovaltsova, D. Coster, R. Schneider, Contribution Plasma Phys. 40 (2000) 423.
[13] V. Rozhansky, S. Voskoboynikov, E. Kaveeva, D. Coster, R. Schneider, Nucl. Fus. 41 (2001) 387.
[14] S.I. Braginskii, in: M.A. Leontovich (Ed.), Rev. Plasma Phys., vol. 1, Consultants Bureau, New York, 1965, p. 205ff.